Nonlinear Dyn (2010) 60: 63–79
DOI 10.1007/s11071-009-9580-2

ORIGINAL PAPER

Modeling intermittent contact for flexible multibody systems

Kishor D. Bhalerao · Kurt S. Anderson

Received: 11 May 2009 / Accepted: 7 August 2009 / Published online: 28 August 2009

Abstract This paper consists of two parts. The first part presents a complementarity based recursive scheme to model intermittent contact for flexible multibody systems. A recursive divide-and-conquer framework is used to explicitly impose the bilateral constraints in the entire system. The presented approach is an extension of the hybrid scheme for rigid multibody systems to allow for small deformations in form of local mode shapes. The normal contact and frictional complementarity conditions are formulated at position and velocity level, respectively, for each body in the system. The recursive scheme preserves the essential characteristics of the contact model and formulates a minimal size linear complementarity problem at logarithmic cost for parallel implementation.

For a certain class of contact problems in flexible multibody systems, the complementarity based time-stepping scheme requires prohibitively small time-steps to retain accuracy. Modeling intermittent contact for this class of contact problems motivated the development of an iterative scheme. The second part of the paper describes this iterative scheme to model unilateral constraints for a multibody system with relatively fewer contacts. The iterative scheme does not require a traditional complementarity formulation and allows the use of any higher order integration methods. A comparison is then made between the traditional complementarity formulation and the presented iterative scheme via numerical examples.

Keywords Intermittent contact · Flexible multibody systems · Complementarity · Divide and conquer · Iterative scheme

K.D. Bhalerao (✉) · K.S. Anderson
Troy, NY 12180, USA
e-mail: bhalek@rpi.edu

K.S. Anderson
e-mail: anderk5@rpi.edu

1 Introduction

Modeling intermittent contact is an important and difficult engineering problem, and a significant amount of literature already exists on the subject. The difficult aspect of modeling contact is developing a physically correct and computationally efficient method. For example, FEM based models [1] are physically accurate but too computationally expensive to be used in most multibody applications. The two other competing families of methods to model intermittent contact in multibody systems are penalty methods and complementarity formulation based methods. In penalty methods, the normal contact force is modeled using a spring–damper model with the frictional force being in the tangential plane at the point of contact. This is a popular approach [2] and is widely used in many multibody applications. However, for certain applications, where the local dynamic behavior of the system

is unimportant, the use of penalty methods is undesirable. For example, in modeling a metal–metal contact, penalty methods capture the ringing of the metal. This results in stable integration time-steps of the order of 10^{-6} being required to capture phenomenon occurring at a much larger time scale (10–20 seconds). In such applications, a better approach to model the contact is to treat it as a kinematic constraint and compute the impulsive changes in state during contact. Such an approach results in a set of complementarity conditions governing the contact process [3–7]. Proximal point formulation [8] is an alternative to the complementarity based methods. In this approach, equivalent variational inequalities are used to represent the corresponding complementarity conditions and an iterative process is used to solve the inequalities. Proximal point formulations are comparable to complementarity based methods in terms of computational time and accuracy of the solution [9]. In the rest of this paper the discussion is limited to complementarity based formulation. Best part of the existing literature is targeted at modeling contacts for rigid bodies. However, for several applications, it is crucial to model the bodies as deformable. Contact modeling for deformable bodies using a complementarity formulation has been described in [9, 10]. In this paper we present a recursive highly parallelizable approach to model unilateral contact in flexible multibody systems using a complementarity formulation. The presented method is an extension of the hybrid scheme for rigid bodies [11] to account for small deformations within the bodies.

The rest of the paper is organized as follows. First, the basics of recursive flexible multibody dynamics in presence of unilateral constraints are described. This is followed by a brief discussion on the complementarity based contact model which is then used to efficiently formulate a traditional linear complementarity problem. Then, the alternative iterative scheme to model intermittent contact is described and a numerical comparison is given between the traditional complementarity formulation and the iterative scheme followed by conclusion.

2 Flexible body dynamics

There are several ways to model a flexible body and a good review of existing methods can be found in [12]. In this paper we use the modal superposition method where large rotations and translations in the system are modeled as rigid body degrees of freedom while the deformation within each body is approximated using superposition of appropriately selected [13] modal shape functions. The divide-and-conquer scheme for flexible multibody systems (FDCA) as presented in [14] is used to describe the dynamics of the system with appropriate modifications to allow for a complementarity formulation. FDCA is briefly described in this section and the interested reader can refer to the original manuscript for more details.

Figure 1 shows a body k of a multibody system in its deformed and undeformed configurations. The body k interacts with its environment via points referred to as handles. Body k has two handles, H_1^k and H_2^k, connecting it to bodies $k-1$ and $k+1$ via joints J^{k-1} and J^k, respectively. A rigid body-fixed reference frame is attached to handle H_1^k and the body k deforms elastically with respect to this frame. The reference frame at handle H_1^k moves relative to the reference frame at handle H_2^{k-1} via the free modes of motion permitted by joint J^{k-1}.

P_0 is an arbitrary differential volume dD in the undeformed configuration and is mapped to P after the body k undergoes the elastic deformation. The displacement vector (δ) between these two points in body-fixed reference frame at H_1^k is expressed in terms of space-dependent shape functions $\{\varphi_i^k\}$ evaluated at P and time-dependent modal coordinates $\{q_i^k\}$ as $\delta = \sum_{i=1}^{\nu_k} \varphi_i^k q_i^k|_P$. Here ν_k is the number of modal coordinates selected for body k. The orientation of body k is then described in terms of generalized coordinates needed for the orientation of the body-fixed reference frame at handle H_1^k and the modal coordinates required for the elastic deformation of the body.

2.1 Divide-and-conquer scheme

The divide-and-conquer algorithm (DCA) for multibody systems is an efficient algorithm to solve the equations of motion for different topologies. Originally presented for rigid bodies [15–17], the method was later extended to include flexible bodies [14]. The framework to manipulate the equations is similar for both rigid and flexible multibody systems and is briefly discussed here.

Consider bodies k and $k+1$ connected together via joint J^k. The goal here is to combine these two bodies to form a fictitious body $k:k+1$ whose equations of

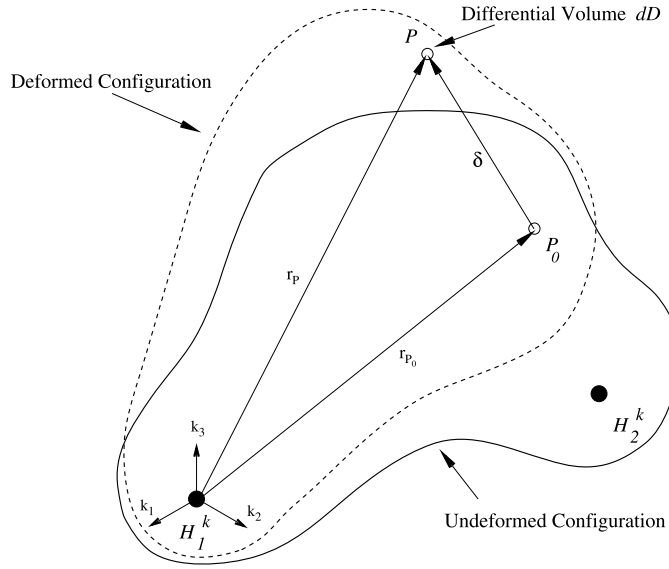

Fig. 1 Deformed and undeformed configurations of body k

motion are in a form identical to that of the individual component bodies k and $k+1$. This is achieved by using the kinematic relationship linking the spatial quantities of the handles connected via joint J^k. This process, also referred to as *assembly*, of combining adjacent bodies is now continued until one has a single all-encompassing body for the entire multibody system. At this point, there are equal number of equations and unknowns. Once the unknown spatial quantities of the terminal handles are computed, the process of combining bodies is reversed. This stage is referred to as the *disassembly* process. In the *disassembly* phase, the known spatial quantities of the terminal handles are used to compute the unknown spatial quantities at the intermediate joints/handles. This is continued until all the unknowns in the system are solved for. In the following discussion we will briefly look at the divide-and-conquer scheme for flexible multibody systems.

2.1.1 Kinematics of body k

Let r_P denote the position vector (see Fig. 1) of the differential volume at P in body k. Let the angular and linear velocities of the differential volume at P in body k, be denoted by ω^P and v^P, respectively. In the subsequent equations, the superscript (or subscript) P is replaced by 1 or 2 to denote the kinematic quantities associated with the handles H_1^k and H_2^k, respectively. The expression for the spatial velocity of this differential element at P ($V_P^k = [\omega^P, v^p]^T$) can then be written as

$$\mathcal{V}_P^k = \left(\mathcal{S}^{r_P}\right)^T \mathcal{V}_1^k + \sum_{i=1}^{\nu_k} \phi_i^k \dot{q}_i^k \Big|_P, \tag{1a}$$

$$\phi_i^k = \left[\psi_i^k, \varphi_i^k\right]^T, \tag{1b}$$

$$\mathcal{S}^{r_P} = \begin{bmatrix} \underline{U} & r_P \times \\ \underline{0} & \underline{U} \end{bmatrix}_{(6\times 6)}. \tag{1c}$$

In (1), ψ^k and φ_i^k refer to the rotational and translational modal shape functions, respectively. $\underline{U}$ is a 3×3 identity matrix. Similarly, if α^P and a^P denote the angular and linear accelerations of the differential volume at P, respectively, then the expression for spatial acceleration ($\mathcal{A}_P^k = [\alpha^P, a^P]^T$) of the differential volume P can be written as

$$\mathcal{A}_P^k = \left(\mathcal{S}^{r_P}\right)^T \mathcal{A}_1^k + \hat{\mathcal{A}}_P^k + \sum_{i=1}^{\nu_k} \phi_i{}^k \ddot{q}_i^k \Big|_P, \tag{2a}$$

$$\hat{\mathcal{A}}_P^k = \begin{bmatrix} \omega^1 \times \sum_{i=1}^{\nu_k} \psi_i{}^k \dot{q}_i{}^k|_P \\ \omega^1 \times (\omega^1 \times r_P) + 2\omega^1 \times \sum_{i=1}^{\nu_k} \varphi_i^k \dot{q}_i{}^k \end{bmatrix}. \tag{2b}$$

2.1.2 Dynamics of body k

Using Kane's method [18], the equations of motion for body k can be written as

$$\begin{bmatrix} \mathbf{\Gamma}_{RR} & \mathbf{\Gamma}_{RF} \\ \mathbf{\Gamma}_{FR} & \mathbf{\Gamma}_{FF} \end{bmatrix} \begin{bmatrix} \mathcal{A}_1^k \\ \ddot{\mathbf{q}}^k \end{bmatrix} - \begin{bmatrix} \gamma_{1R} \\ \gamma_{1F} \end{bmatrix} \mathcal{F}_1^k$$

$$-\begin{bmatrix}\gamma_{2R}\\ \gamma_{2F}\end{bmatrix}\mathcal{F}_2^k+\begin{bmatrix}\beta_R\\ \beta_F\end{bmatrix}$$
$$+\begin{bmatrix}\kappa_{1R}\\ \kappa_{1F}\end{bmatrix}\lambda_N^k+\begin{bmatrix}\kappa_{2R}\\ \kappa_{2F}\end{bmatrix}\lambda_F^k=\begin{bmatrix}0\\ 0\end{bmatrix}. \tag{3}$$

In (3), $\ddot{\mathbf{q}}^k$ contains all the modal coordinates for the body k. Also, $\mathcal{F}_1^k=[\tau_1^k, f_1^k]^T$ and $\mathcal{F}_2^k$ are the spatial constraint forces acting on handles H_1^k and H_2^k, respectively. The terms λ_N and λ_F are the unknown normal contact force and the corresponding frictional force acting on the body k, respectively. The subscripts (R, RR) and (F, FF) are used to denote the rigid and flexible modes of motion, respectively, while the subscripts (RF, FR) are used to denote the coupling between the flexible and rigid body modes of motion. The terms β_R and β_F contain all the known forces acting on the body k including the stiffness and damping terms. From (3), the expression for $\ddot{\mathbf{q}}^k$ can be obtained as

$$\ddot{\mathbf{q}}^k=\mathcal{G}_1\mathcal{A}_1^k+\mathcal{G}_2\mathcal{F}_1^k+\mathcal{G}_3\mathcal{F}_2^k+\mathcal{G}_4+\mathcal{G}_5\lambda_N^k+\mathcal{G}_6\lambda_F^k. \tag{4}$$

Henceforth $\mathcal{G}_i$ would refer to intermediate known quantities. Substituting (4) into (3), an expression for the spatial acceleration of handle H_1^k can be obtained in terms of the unknown spatial constraint forces acting on handles H_1^k and H_2^k. Also, using the kinematic relationship given in (2), the expression for the spatial acceleration of handle H_2^k can be obtained. Thus, the equations for spatial acceleration for handles H_1^k and H_2^k can be written as

$$\mathcal{A}_1^k=\zeta_{11}^k\mathcal{F}_1^k+\zeta_{12}^k\mathcal{F}_2^k+\zeta_{13}^k+\zeta_{14}^k\lambda_N^k+\zeta_{15}^k\lambda_F^k, \tag{5a}$$
$$\mathcal{A}_2^k=\zeta_{21}^k\mathcal{F}_1^k+\zeta_{22}^k\mathcal{F}_2^k+\zeta_{23}^k+\zeta_{24}^k\lambda_N^k+\zeta_{25}^k\lambda_F^k. \tag{5b}$$

Equation (5) is henceforth referred to as the two-handle equation for body k. Thus, (4) and (5) together describe the dynamics for body k. Similarly, the two-handle equation for body $k+1$ can be written as

$$\mathcal{A}_1^{k+1}=\zeta_{11}^{k+1}\mathcal{F}_1^{k+1}+\zeta_{12}^{k+1}\mathcal{F}_2^{k+1}+\zeta_{13}^{k+1}+\zeta_{14}^{k+1}\lambda_N^{k+1}+\zeta_{15}^{k+1}\lambda_F^{k+1}, \tag{6a}$$
$$\mathcal{A}_2^{k+1}=\zeta_{21}^{k+1}\mathcal{F}_1^{k+1}+\zeta_{22}^{k+1}\mathcal{F}_2^{k+1}+\zeta_{23}^{k+1}+\zeta_{24}^{k+1}\lambda_N^{k+1}+\zeta_{25}^{k+1}\lambda_F^{k+1}. \tag{6b}$$

We next look at the *assembly–disassembly* process.

Assembly As discussed before, the goal in the assembly process is to combine the two adjacent bodies to form a fictitious body as shown in Fig. 2, by using the kinematic relationship linking the spatial acceleration

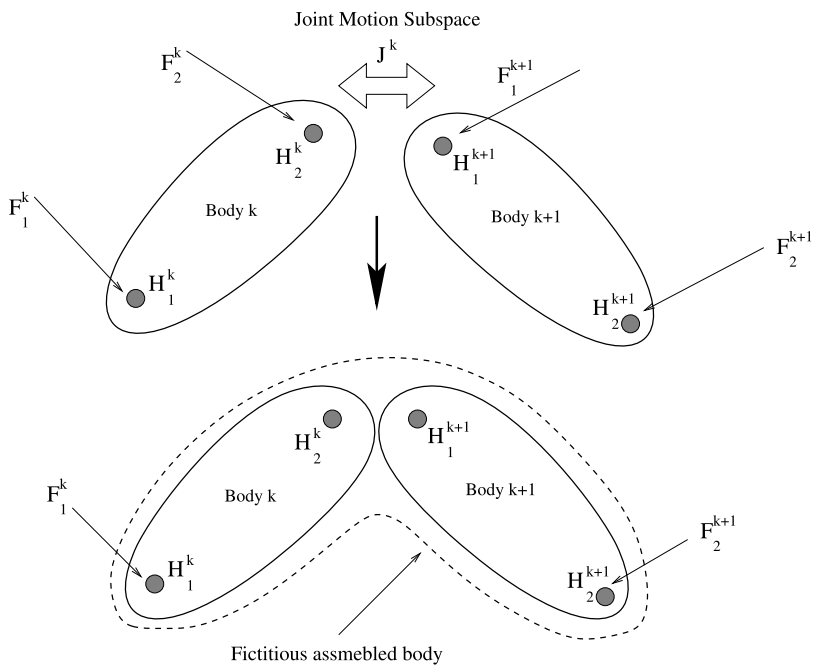

Fig. 2 Fictitious body formed in the assembly process

of the handles connected via joint J^k. The kinematic relationship for joint J^k can be written as

$$\mathcal{A}_1^{k+1} - \mathcal{A}_2^k = P^{J^k}\dot{\mathbf{u}}^{J^k} + \mathcal{A}_t^{J^k}. \tag{7}$$

In (7), P^{J^k} is a $6 \times f^k$ matrix, whose columns correspond to the spatial partial velocity of the f^k degree-of-freedom joint J^k and $\dot{\mathbf{u}}^{J^k}$ is a list of time derivative of generalized speeds of the joint. $\mathcal{A}_t^{J^k}$ contains all remaining acceleration terms which are completely known. Substituting the expressions for $\mathcal{A}_2^k$ and $\mathcal{A}_1^{k+1}$ from (5b) and (6a), respectively, and using the fact that $\mathcal{F}_2^k = -\mathcal{F}_1^{k+1}$, after some manipulation, the expression for spatial constraint force acting on handle H_2^k can be written as

$$\begin{aligned}\mathcal{F}_2^k = {} & \mathcal{G}_7\mathcal{F}_1^k + \mathcal{G}_8\mathcal{F}_2^{k+1} + \mathcal{G}_9 + \mathcal{G}_{10}\lambda_N^k + \mathcal{G}_{11}\lambda_F^k \\ & + \mathcal{G}_{12}\lambda_N^{k+1} + \mathcal{G}_{13}\lambda_F^{k+1}.\end{aligned} \tag{8}$$

Substituting (8) into (5a) and (6b), the two-handle equation for the combined fictitious body can be written as

$$\begin{aligned}\mathcal{A}_1^k = {} & \xi_{11}\mathcal{F}_1^k + \xi_{12}\mathcal{F}_2^{k+1} + \xi_{13} \\ & + \xi_{14}\boldsymbol{\Lambda}_{\mathbf{N}}^{\mathbf{k:k+1}} + \xi_{15}\boldsymbol{\Lambda}_{\mathbf{F}}^{\mathbf{k:k+1}},\end{aligned} \tag{9a}$$

$$\begin{aligned}\mathcal{A}_2^{k+1} = {} & \xi_{21}\mathcal{F}_1^k + \xi_{22}\mathcal{F}_2^{k+1} + \xi_{23} \\ & + \xi_{24}\boldsymbol{\Lambda}_{\mathbf{N}}^{\mathbf{k:k+1}} + \xi_{25}\boldsymbol{\Lambda}_{\mathbf{F}}^{\mathbf{k:k+1}}.\end{aligned} \tag{9b}$$

In (9), $\boldsymbol{\Lambda}_{\mathbf{N}}^{\mathbf{k:k+1}}$ and $\boldsymbol{\Lambda}_{\mathbf{F}}^{\mathbf{k:k+1}}$ are lists containing the normal contact force and corresponding frictional force, respectively, acting on bodies k and $k+1$. This process is now continued until we get a single all-encompassing fictitious body for the entire system. If the multibody system consists of nb bodies, then the two-handle equation for the entire assembly can be written as

$$\begin{aligned}\mathcal{A}_1^1 = {} & \xi_{11}^{1:nb}\mathcal{F}_1^1 + \xi_{12}^{1:nb}\mathcal{F}_2^{nb} + \xi_{13}^{1:nb} \\ & + \xi_{14}^{1:nb}\boldsymbol{\Lambda}_{\mathbf{N}}^{\mathbf{1:nb}} + \xi_{15}^{1:nb}\boldsymbol{\Lambda}_{\mathbf{F}}^{\mathbf{1:nb}},\end{aligned} \tag{10a}$$

$$\begin{aligned}\mathcal{A}_2^{nb} = {} & \xi_{21}^{1:nb}\mathcal{F}_1^1 + \xi_{22}^{1:nb}\mathcal{F}_2^{nb} + \xi_{23}^{1:nb} \\ & + \xi_{24}^{1:nb}\boldsymbol{\Lambda}_{\mathbf{N}}^{\mathbf{1:nb}} + \xi_{25}^{\mathbf{1:nb}}\boldsymbol{\Lambda}_{\mathbf{F}}^{\mathbf{1:nb}}.\end{aligned} \tag{10b}$$

The two-handle equations for the entire assembly can now be solved for different constraints on the terminal handles following the procedure described in [17] to obtain the expression for the spatial quantities at the terminal handles. Thus, the expression for the spatial constraint force acting on the terminal handles can be written as

$$\mathcal{F}_1^1 = \mathcal{G}_{14} + \mathcal{G}_{15}\boldsymbol{\Lambda}_{\mathbf{N}}^{\mathbf{1:nb}} + \mathcal{G}_{16}\boldsymbol{\Lambda}_{\mathbf{F}}^{\mathbf{1:nb}}, \tag{11a}$$

$$\mathcal{F}_2^{nb} = \mathcal{G}_{17} + \mathcal{G}_{18}\boldsymbol{\Lambda}_{\mathbf{N}}^{\mathbf{1:nb}} + \mathcal{G}_{19}\boldsymbol{\Lambda}_{\mathbf{F}}^{\mathbf{1:nb}}. \tag{11b}$$

Using (11), (10) can be reduced to the following form:

$$\mathcal{A}_1^1 = \mathcal{G}_{20} + \mathcal{G}_{21}\boldsymbol{\Lambda}_{\mathbf{N}}^{\mathbf{1:nb}} + \mathcal{G}_{22}\boldsymbol{\Lambda}_{\mathbf{F}}^{\mathbf{1:nb}}, \tag{12a}$$

$$\mathcal{A}_2^{nb} = \mathcal{G}_{23} + \mathcal{G}_{24}\boldsymbol{\Lambda}_{\mathbf{N}}^{\mathbf{1:nb}} + \mathcal{G}_{25}\boldsymbol{\Lambda}_{\mathbf{F}}^{\mathbf{1:nb}}. \tag{12b}$$

Disassembly In the disassembly process, the goal is to compute the spatial quantities at intermediate handles regarding $\boldsymbol{\Lambda}_{\mathbf{N}}^{\mathbf{1:nb}}$ and $\boldsymbol{\Lambda}_{\mathbf{F}}^{\mathbf{1:nb}}$ as parameters. Consider the fictitious assembly $k : k+1$ as shown in Fig. 2. If the spatial quantities at the terminal handles H_1^k and H_2^{k+1} are known in terms of the parameters $\boldsymbol{\Lambda}_{\mathbf{N}}^{\mathbf{1:nb}}$ and $\boldsymbol{\Lambda}_{\mathbf{F}}^{\mathbf{1:nb}}$, then these can be used in the two-handle equations of the constituent bodies k and $k+1$ to obtain the spatial constraint force and acceleration of handles H_2^k and H_2^{k+1}. Now, if we were to imagine the bodies k and $k+1$ themselves as assemblies or subsystems, then the spatial quantities of their terminal handles are now known and the *disassembly* process can continue until all the unknown quantities in the system are computed in terms of the contact parameters. Thus at the end of the *disassembly* process, the spatial acceleration and constraint force for a body k can be written as

$$\mathcal{A}_1^k = \mathcal{G}_{26} + \mathcal{G}_{27}\boldsymbol{\Lambda}_{\mathbf{N}}^{\mathbf{1:nb}} + \mathcal{G}_{28}\boldsymbol{\Lambda}_{\mathbf{F}}^{\mathbf{1:nb}}, \tag{13a}$$

$$\mathcal{A}_2^k = \mathcal{G}_{29} + \mathcal{G}_{30}\boldsymbol{\Lambda}_{\mathbf{N}}^{\mathbf{1:nb}} + \mathcal{G}_{31}\boldsymbol{\Lambda}_{\mathbf{F}}^{\mathbf{1:nb}}, \tag{13b}$$

$$\mathcal{F}_1^k = \mathcal{G}_{32} + \mathcal{G}_{33}\boldsymbol{\Lambda}_{\mathbf{N}}^{\mathbf{1:nb}} + \mathcal{G}_{34}\boldsymbol{\Lambda}_{\mathbf{F}}^{\mathbf{1:nb}}, \tag{13c}$$

$$\mathcal{F}_2^k = \mathcal{G}_{35} + \mathcal{G}_{36}\boldsymbol{\Lambda}_{\mathbf{N}}^{\mathbf{1:nb}} + \mathcal{G}_{37}\boldsymbol{\Lambda}_{\mathbf{F}}^{\mathbf{1:nb}}. \tag{13d}$$

Using (13) in (4), $\ddot{\mathbf{q}}^k$ can be written as

$$\ddot{\mathbf{q}}^k = \mathcal{G}_{38} + \mathcal{G}_{39}\boldsymbol{\Lambda}_{\mathbf{N}}^{\mathbf{1:nb}} + \mathcal{G}_{40}\boldsymbol{\Lambda}_{\mathbf{F}}^{\mathbf{1:nb}}. \tag{14}$$

Since at this point the contact forces are unknown, the matrices $\mathcal{G}_{26}$ to $\mathcal{G}_{40}$ must be stored for each body to be used later when the contact force is computed using a complementarity formulation. Equations (13) and (14) are in a form suitable to allow a traditional complementarity formulation which we discuss in the following section.

3 Contact model

The contact model consists of a set of complementarity conditions enforcing the kinematic non-penetration constraint with dry friction at the point of contact. The contact model described in this paper is identical to the one described in [19] and is only briefly discussed here.

Consider two bodies approaching each other with impending contact as shown in Fig. 3. The minimal distance between the two approaching bodies is represented by g_N. It is assumed that a signed g_N can be calculated by existing softwares given the state of the system. Then the non-penetration constraint between the two bodies can simply be stated as $g_N \geq 0$. If the corresponding normal contact force between the two bodies is represented by λ_N, then the complementarity relationship between the normal contact force and minimal distance can be stated as $0 \leq g_N \perp \lambda_N \geq 0$. Next, the frictional force λ_F at the point of contact lies in the tangential plane opposing the relative tangential motion. In addition to this, the magnitude of the frictional force must satisfy the relationship $\lambda_F \leq \mu\lambda_N$, where μ is the coefficient of friction. In order to avoid a nonlinear complementarity problem, a linear approximation of the friction cone is used resulting in the contact force which takes the form

$$\mathcal{F} = \left\{\lambda_N n + \lambda_F \mathcal{D}_c \mid \lambda_N \geq 0,\ \lambda_F \geq 0,\ e^T \lambda_F \leq \mu\lambda_N\right\}. \tag{15}$$

In (15), $\mathcal{D}_c$ is a matrix whose columns consist of η unit vectors positively spanning the possible directions of frictional force at the point of contact. n is the normal at the point of contact and $e = [1, 1, \ldots, 1]^T \in \Re^\eta$. Next we proceed to writing the complementarity conditions to calculate the normal contact force and tangential frictional force.

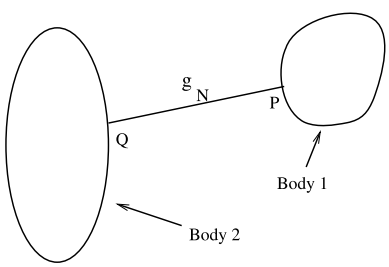

Fig. 3 Impending contact

3.1 Complementarity formulation

Let the t^l denote the current time. Then, to ensure non-penetration constraint in the time step $t^l - t^{l+1}$, the complementarity condition which must be enforced is

$$0 \leq g_N^{l+1} \perp \lambda_N^{l+1} \geq 0. \tag{16}$$

In (16), λ_N^{l+1} is the normal contact force acting in the time step $t^l - t^{l+1}$. g_N^{l+1} is approximated using the following expression:

$$g_N^{l+1} = g_N^l + h\, n \cdot v_r^{l+1} + \frac{\delta g_N}{\delta t} + \epsilon. \tag{17}$$

In (17), v_r is the relative contact velocity vector, $\frac{\delta g_N}{\delta t}$ accounts for the prescribed motion between the two bodies in normal direction, h is the constant time-step of integration and ϵ is the first-order error.

The frictional force requires two sets of complementarity conditions, the first one to set the direction opposing the relative motion in tangential plane at the point of contact and the second set to ensure that the magnitude of the frictional force lies within the linearized friction cone. These can be written as

$$0 \leq \mathcal{S}^{l+1} e + \mathcal{D}_c^T \cdot \left(v_r^{l+1} + \frac{\delta g_T}{\delta t}\right) \perp \lambda_F^{l+1} \geq 0, \tag{18a}$$

$$0 \leq \mu\lambda_N^{l+1} - e^T \lambda_F^{l+1} \perp \mathcal{S}^{l+1} \geq 0. \tag{18b}$$

In (18), $\mathcal{S}$ is an approximation of the relative tangential contact speed and $\frac{\delta g_T}{\delta t}$ is the prescribed motion in the tangential direction. Equation (18a) sets the direction of the frictional force while (18b) ensures that the magnitude of the frictional force does not exceed $\mu\lambda_N$.

The complementarity conditions in the current form describe an inelastic contact. It is easy to extend these conditions to include coefficient of restitution based models as has been described in [11]. However, such an approach is most appropriate only when the behavior of the body is close to that of rigid bodies. It is shown in [20, 21] that the coefficient of restitution in case of impulsive response of a flexible multibody system has a different interpretation than a rigid body impact and on use of sufficient number of modal shape functions, the actual value of this coefficient becomes irrelevant. In the present work, it is assumed that all the important modal shape functions are included while deriving the equations of motion and the energy loss is achieved via structural damping instead of a restitution based model [22].

3.2 Linear complementarity problem for intermittent contact

Equations (16) and (18) must be solved along with equations of motion for each body with impending or current contact. Clearly, an expression for v_r^{l+1} in terms of the state at time t^l is required to solve the complementarity conditions. This is obtained in the following manner.

Following the procedure described in Sect. 2, the expression for $\ddot{\mathbf{q}}^k$ (see (14)) and the spatial acceleration (see (13)) of all the handles of the constituent bodies of a flexible multibody system can be obtained in terms of the unknown parameters λ_N^k and λ_F^k. Using (13) and (14), (2) can be reduced to the following form:

$$\mathcal{A}_P^k = \mathcal{G}_{41} + \mathcal{G}_{42}\mathbf{\Lambda_N^{1:nb}} + \mathcal{G}_{43}\mathbf{\Lambda_F^{1:nb}}. \tag{19}$$

The location of point P on body k, in this case, corresponds to the point of impending contact and is already known based on the state of the system at time t^l. Then (19) can be discretized as

$${}^{l+1}\mathcal{V}_P^k = {}^{l}\mathcal{V}_P^k + h\big(\mathcal{G}_{41} + \mathcal{G}_{42}\mathbf{\Lambda_N^{1:nb}} + \mathcal{G}_{43}\mathbf{\Lambda_F^{1:nb}}\big). \tag{20}$$

Then ${}^k v_r^{l+1}$ can be obtained from (20) by premultiplying both sides of the equation by matrix $D = [Z \quad U]_{3\times 6}$, where Z and U are zero and identity matrices respectively of size 3×3. The expression for ${}^k v_r^{l+1}$ can then be written as

$${}^k v_r^{l+1} = \mathcal{G}_{44} + \mathcal{G}_{45}\mathbf{\Lambda_N^{1:nb}} + \mathcal{G}_{46}\mathbf{\Lambda_F^{1:nb}}. \tag{21}$$

While computing an expression for the relative contact velocity vector, it was assumed that the obstacle was stationary. This however is not a limiting assumption and a similar calculation can be done for a moving obstacle and the expression for relative contact velocity vector modified accordingly.

The procedure described above can be used for all bodies with impending contact to calculate the relative contact velocity vector. These equations can be summarized as

$$\mathbf{^{1:nb}v_r^{l+1}} = \mathcal{G}_{\mathbf{47}} + \mathcal{G}_{\mathbf{48}}\mathbf{\Lambda_N^{1:nb}} + \mathcal{G}_{\mathbf{49}}\mathbf{\Lambda_F^{1:nb}}. \tag{22}$$

In (22), $\mathbf{^{1:nb}v_r^{l+1}}$ is a list of relative contact velocity vectors for the impending contacts of all the bodies in the system. The complementarity conditions given in (16) and (18) can now be written for each contact, resulting in the following linear complementarity problem (LCP) for the entire system:

$$0 \le \begin{bmatrix} \mathbf{\Lambda_N} \\ \mathbf{\Lambda_F} \\ \mathcal{S} \end{bmatrix}_{1:nb}^{l+1} \perp \left(\begin{bmatrix} h\mathbf{n}\mathcal{G}_{48} & h\mathbf{n}\mathcal{G}_{49} & \underline{\mathbf{0}} \\ \mathcal{D}_\mathbf{c}^\mathbf{T}\mathcal{G}_{48} & \mathcal{D}_\mathbf{c}^\mathbf{T}\mathcal{G}_{49} & \mathbf{e} \\ \mu & -\mathbf{e}^T & \underline{\mathbf{0}} \end{bmatrix} \times \begin{bmatrix} \mathbf{\Lambda_N} \\ \mathbf{\Lambda_F} \\ \mathcal{S} \end{bmatrix}_{1:nb}^{l+1} + \begin{bmatrix} \mathbf{g_N} + h\mathbf{n}\mathcal{G}_{47} + \frac{\delta \mathbf{g_N}}{\delta t} \\ \mathcal{D}_\mathbf{c}^\mathbf{T}(\mathcal{G}_{47} + \frac{\delta \mathbf{g_T}}{\delta t}) \\ \underline{\mathbf{0}} \end{bmatrix} \right) \ge 0. \tag{23}$$

In (23), μ is a diagonal matrix with diagonal entries corresponding to the coefficients of friction for each contact. Equation (23) is in the standard LCP form and can be solved for using any of the existing well established algorithms to yield λ_N^k and λ_F^k for the entire system. These values can now be used in (20) to obtain the spatial velocity of all the handles in the multibody system at the next time step. Similarly, a discretized form of (14) can be used to obtain the time derivative of the modal coordinates (${}^{l+1}\dot{q}^k$) at the next time step. Following this procedure, the simulation can now proceed.

3.3 Computational efficiency

Simulating intermittent contact involves two steps, the first being the formulation of an LCP (or mixed complementarity problem (MCP)) and the second involves solving the LCP using established algorithms. Of these two steps, solving the LCP is the slowest step which in turn dictates the speed of the simulation. In the approach presented in [10], the bilateral constraints are implicitly imposed and appended to the equations of motion for the entire system. In flexible multibody systems involving multiple bilateral constraints, the size of the resulting MCP is then directly dependent on the number of bilateral constraints. This in turn significantly increases the cost of solving the MCP. The size of the complementarity problem to be solved at each time step can be decreased by eliminating the system-wide mass matrix and the constraint equations resulting in a minimal size LCP. While formulating an LCP from the MCP, an $O(n^3)$ expense is encountered at each time step, where n is the number of generalized coordinates associated with the bilateral constraints in the system. This can be prohibitive for certain applications.

The method presented in this paper is specially advantageous when there are bilateral constraints in the system. In this work, the bilateral constraints in the system are imposed exactly via use of relative joint coordinates. The formulation of LCP from (13) which is obtained at the end of the *assembly–disassembly* process does not require any additional computational expense. Potentially, the largest matrix which must be inverted in FDCA is $\mathbf{\Gamma}_{FF}$ (see (3)) which is a $\nu^k \times \nu^k$ matrix. This matrix, however, is time invariant and the cost of its inversion only adds to the preprocessing cost. The other matrix manipulations in (4) involve multiplying the matrices of dimension $\nu_k \times \nu_k$ and $\nu_k \times 6$ which is a $O(\nu^2)$ process. The divide-and-conquer framework to yield the relationship given in (13) in itself is of logarithmic complexity [14] for parallel implementation and is an $O(\log(n))$ process. Thus the LCP can be formulated in a minimal cost of $O(\log(n) + \nu^2)$.

The substructured approach of the DCA framework can be effectively exploited in situations where there is an impending contact on only a few bodies in the system. For example, consider a flexible multibody system having 8 bodies as shown in Fig. 4, with impending contact on bodies 3 and 7. During the assembly process, the bodies which do not have an impending contact are assembled first to form sub-assemblies. The assembly process is now continued to form a single fictitious body for the entire system. Once the two-handle equations for the entire system are solved in terms of the unknown contact force parameters, the disassembly process can now be stopped at the stage when the spatial quantities of the handles on the bodies involving a unilateral constraint are known in terms of the contact force parameters. In the current example, the disassembly process can be stopped at the first step as shown in Fig. 4. The data generated by this step of the disassembly process is sufficient to formulate and solve the LCP given in (23). Once the LCP is solved, the contact force is completely known and the disassembly process can now continue without having to store the matrices $\mathcal{G}_{26} \cdots \mathcal{G}_{40}$ for the remaining bodies. This helps in minimizing the data that must be stored (see (13), (14)) at each time step. Additionally, during the course of the simulation, if the impending contact shifts from one body to another, the order in which the bodies are *assembled* and *disassembled* can easily be changed. Such a capability is easy to build into the simulation code due to the underlying substructured approach used to formulate the LCP.

4 An alternative approach to contact problems

4.1 Motivation

The traditional complementarity formulations or time-steppers for intermittent contact are almost without exception first-order integration methods (an iterative complementarity formulation resulting in higher order integration methods is described in [9, 22]). These methods formulate an LCP whose solution yields the integral of the contact force acting over the fixed time-step. The resulting impulsive contact force (I_c) is such that it avoids interpenetration between interacting bodies. However, since a first-order discretization (see (20)) is used for the equations of motion to calculate the contact impulse (I_c), it can be written as $I_c = \int F_c \, dt \approx F_c \Delta t$, where F_c is the constant contact force acting over the fixed time-step Δt. From this, it can be directly argued that, although the LCP solvers compute the values of contact impulse acting over the fixed time-step, the effect of this impulse is identical to that of a constant force $F_c = I_c/\Delta t$ acting on the system over the fixed time-step for the se-

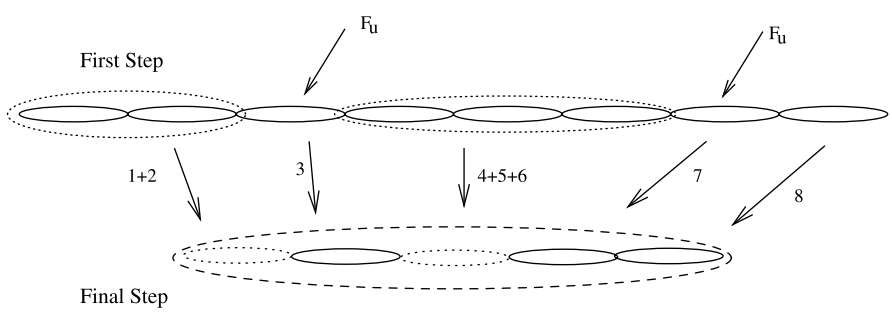

Fig. 4 Order of *assembly* is modified to minimize data storage

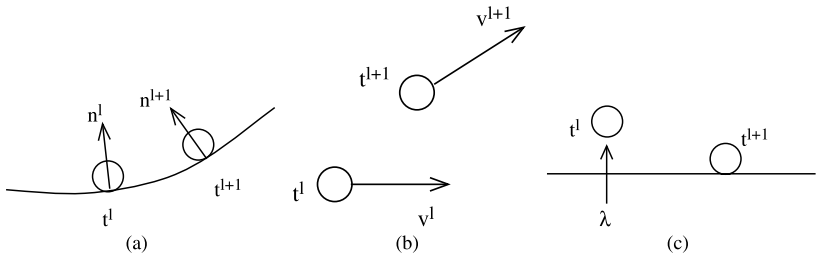

Fig. 5 A time step cannot be large due to contact considerations

lected first-order discretization of the equations of motion.

The size of the fixed time-step has some additional constraints due to the nature of the contact problem. For example, in Fig. 5, the initial and final positions of a body during the time step $t^l - t^{l+1}$ are shown for three different cases. Figure 5(a) shows the case when the contact normal changes over the course of the current time-step. Similarly, in Fig. 5(b), the direction of relative motion changes during the current time-step. As discussed before, complementarity formulations require that the contact force during the current time-step be applied in a fixed direction. This in turn requires that the size of the selected time-step be sufficiently small so that the contact normal and the direction of relative motion during contact does not change significantly during the course of the time step. The other case (Fig. 5(c)) is when the contact is established in the current time-step. If the time step is too large, the contact force gets applied on the system too soon, which is undesirable. Thus, the time steps during the actual contact have to be sufficiently small to retain the accuracy of the simulation. The use of small time-steps with these contact considerations in turn reduces the error introduced into the equations of motion due to a first-order discretization.

The solution to the LCP ensures that the contact forces satisfy the complementarity conditions (see (16) and (18)) which in turn depend upon the expression for the relative contact velocity (v_r^{l+1}) at time t^{l+1}. This expression is obtained by a first-order discretization of the expression for the acceleration at the point of contact (see (19)–(21)). Thus, the accuracy of the contact forces obtained is limited by this first-order discretization. For small time-steps, this approach gives satisfactory results for most applications. However, as previously discussed, for certain applications, it is desirable to model deformations occurring within the bodies via superposition of local modal shape functions. Some of these mode shapes could potentially have a high natural frequency which could result in incorrect computation of contact forces. For example, consider a system with n generalized coordinates (q) and corresponding generalized speeds (u). Then, the relative acceleration of the point of contact can be written as $\frac{dv_r}{dt} = f(t, q, u)$. Using a Taylor series expansion, the expression for v_r^{l+1} can be written as

$$v_r^{l+1} = v_r^l + f\Delta t + \frac{\Delta t^2}{2!}\frac{df}{dt} + \frac{\Delta t^3}{3!}\frac{d^2 f}{dt^2} + \cdots, \quad (24a)$$

$$\frac{df}{dt} = \frac{\partial f}{\partial t} + \sum_{i=1}^{n} \frac{\partial f}{\partial q_i}\frac{dq_i}{dt} + \sum_{i=1}^{n} \frac{\partial f}{\partial u_i}\frac{du_i}{dt}. \quad (24b)$$

For the high frequency modes, the time derivatives of q_i and u_i are significant and can no longer be ignored. If these terms are not included in the expression for v_r^{l+1}, the computed contact force could differ significantly from the correct value. Calculating $\frac{\partial f}{\partial q}$ and $\frac{\partial f}{\partial u}$ for flexible multibody system with bilateral constraints is a non-trivial task.

Thus, certain contact problems in flexible multibody systems motivated the development of an alternative approach which would not depend on a first-order discretization to obtain an expression for v_r^{l+1} and allow the use of higher order integration routines to improve accuracy. The iterative scheme is specially targeted at applications with relatively fewer contacts as encountered in certain applications in robotics and biomechanics, among others. The applications of the alternative iterative scheme are not limited to the flexible domain and it can be readily applied to rigid body contact problems. The iterative scheme is however not optimal for contact problems in which a simultaneous frictional contact is possible between any two bodies in the system. We next look at the iterative scheme and numerically compare the results with the traditional complementarity problems.

4.2 Iterative scheme

This scheme consists of three main steps. The first step involves iteratively computing the required contact force, given the other forces acting on the system, to prevent interpenetration. The second step involves calculating the regimes of motion (*stick* or *slide*) based on the calculated normal force and the third step involves calculating the corresponding frictional force. These three steps are repeated until the convergence criteria is met.

4.2.1 Normal contact force

In the traditional LCP formulations, the magnitude of the contact force required to prevent interpenetration is unknown. This makes the forward dynamics problem implicit in nature. To make use of higher order integration methods, we assume a value for the normal contact force λ_N and then the forward dynamics problem becomes explicit. If x is the state vector for the entire system, a function $\dot{x} = f(t, x^l, \lambda_N, \lambda_F)$ can be written using any appropriate method. λ_N and λ_F are assumed to be either zero or assigned a value from the previous iteration. The value of λ_F is left unchanged in the first step and λ_N is computed iteratively as follows. The system is advanced from current time t^l to t^{l+1} using any of the higher order integration methods. At time t^{l+1}, the distance function g_N^i (see Fig. 3) is computed, where the superscript i is the iteration counter. Interference will be indicated by a negative value of g_N^i. Next, a new value of λ_N^{i+1} is assumed and the system is again advanced from time t^l to t^{l+1}, as before. After the first two iterations we have two sets of the ordered pair $(\lambda_N,\ g_N)^i$. The next value of λ_N, corresponding to $g_N = 0$, is calculated first by a linear interpolation and subsequently by polynomial approximation and the process is repeated until the calculated g_N is less than the preselected tolerance levels. The normal along which the contact force is applied is recalculated based on the state vector generated at time t^{l+1} in each iteration. This process is equivalent to the *nonlinear case* described in [19].

While it is not possible to mathematically prove convergence for the above process, it has been observed that these iterations converge rapidly to yield a value of λ_N which results in $g_N \approx 0$. The explanation for the observed behavior is as follows. Due to reasons described in the previous section, the time step during contact must be sufficiently small. One direct consequence of using a small time-step is that the behavior of the system within this time step is largely linear. While, the first two values of λ_N must be assumed or taken from previous step, it has been observed that a single linear interpolation is usually sufficient to yield the correct λ_N corresponding to $g_N \approx 0$. Figure 6 gives the graphical representation of the iterative approach used to compute λ_N.

4.2.2 Regimes of motion

The contact force obtained from the iterative scheme given in Fig. 6 corresponds to frictionless case when $\lambda_F = 0$. The tangential velocity (v_t^{l+1}) at the point of contact then gives the direction of impending motion in absence of friction at time t^{l+1}. The basic idea of finding the regime of motion is as follows. Apply a frictional force $\lambda_F = \mu\lambda_N$ in a direction opposing the impending motion and then recompute the relative tangential velocity at time t^{l+1}. If the recomputed relative tangential velocity (v_t^{l+1}) at the point of contact has a positive projection on the applied frictional force, then this is a case of *sticking* and $\lambda_F < \mu\lambda_N$, else one gets a *sliding* regime with $\lambda_F = \mu\lambda_N$. For the first iteration with $\lambda_F = 0$, when either v_t^l or v_t^{l+1} is zero, the direction of frictional force is chosen opposing the direction of the non-zero tangential velocity. In the situation when both v_t^l and v_t^{l+1} are non-zero, the direction of frictional force is chosen to oppose the mean direction of relative tangential velocities during the time step. Similarly, if both v_t^l and v_t^{l+1} are zero for $\lambda_F = 0$, then the frictional force acting at the point of contact is zero. For the *sliding* regime, this direction of applied frictional force is kept fixed during subsequent iterations.

If the detected regime is *sliding*, no further treatment is required and the current estimate of $\lambda_F = \mu\lambda_N$ is used as an external force and iterations are continued from the first step. If the detected regime is *sticking*, obtaining an estimate for the frictional force requires some additional treatment.

4.2.3 Sticking frictional force

To calculate the frictional force which will prevent any relative motion in the tangential direction at the point of contact, the following two cases are considered.

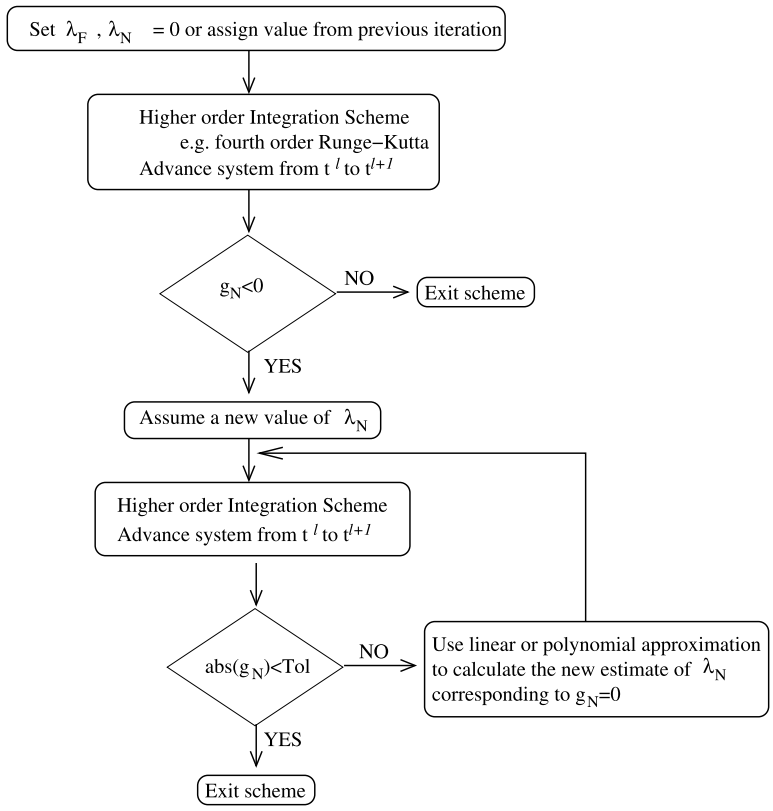

Fig. 6 Iterative approach to obtain an estimate of the normal contact force λ_N for the time step t^l-t^{l+1}

$v_t^l = 0$: If the tangential velocity of the point of contact at time t^l is zero, then to ensure a no-slip condition, the additional constraint of a zero tangential acceleration at the point of contact must be enforced. The goal is then to calculate an external frictional force which will ensure a zero tangential acceleration at the point of contact. If the body under consideration does not have any additional bilateral constraints, computing the frictional force corresponding to zero tangential acceleration at point of contact is straightforward. For a body k with additional bilateral constraints (see Fig. 7), the equation of the spatial acceleration ($\mathcal{A}^P$) at the point of contact P can be written as

$$\mathcal{A}^P = \mathcal{G}_{50}\mathcal{F}_1^k + \mathcal{G}_{51}\mathcal{F}_2^k + \mathcal{G}_{52}\lambda_F + \mathcal{G}_{53}. \tag{25}$$

Define a matrix D^p whose columns form the basis of the tangential plane at the point of contact. Then $(D^p)^T\mathcal{A}^P = \mathbf{0}$ is the tangential acceleration at the point of contact. Using this relationship, the frictional force can be expressed in terms of the bilateral constraint forces as

$$\lambda_F = \mathcal{G}_{54}\mathcal{F}_1^k + \mathcal{G}_{55}\mathcal{F}_2^k + \mathcal{G}_{56}. \tag{26}$$

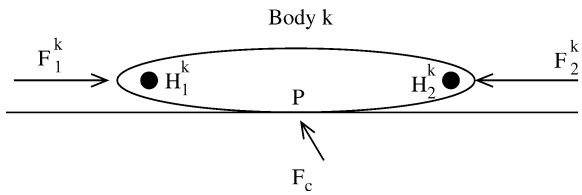

Fig. 7 No-slip condition at point P

Equation (26) can now be used to obtain the two-handle equation for the body k and initiate the divide-and-conquer scheme to compute the state derivatives for the entire system and advance the simulation from time t^l to t^{l+1}. During this process, an estimate for λ_F is obtained corresponding to a zero relative tangential acceleration at the point of contact which can be used an in input in the first step.

$v_t^l \neq 0$: In this case, the initial tangential velocity is non-zero. However, during the current time-step, the frictional force is sufficient to prevent any relative motion in tangential direction. This suggests that the relative tangential velocity of the body at the point of con-

tact is instantaneously reduced to zero. This amounts to a applying a true frictional impulse (I_F) at the point of contact which would remove any relative tangential velocity at the point of contact. Computing this frictional impulse for a body which does not have any bilateral constraints is straightforward. For a system of bodies connected via bilateral constraints, the frictional impulse can be computed using the procedure described in [23] and [24] for rigid and flexible multibody systems respectively. Once the relative tangential velocity of the body is reduced to zero, the procedure described previously can be used to advance the system from time t^l to t^{l+1} to obtain an estimate for λ_F. Thus, having an estimate for I_F and λ_F, the first step can now be repeated.

The entire approach can be briefly summarized as follows. In the first step, an estimate for λ_N is obtained via a linear or polynomial approximation (see Fig. 6). During the first step, the value of the frictional force is assumed to be constant. The estimate of λ_N from the first step is then set as constant for the second and third steps. In the second step, the regime of motion is calculated by applying a frictional force corresponding to the estimate of the normal contact force obtained in the first step. If the detected regime is *sliding*, the obtained estimate of λ_F is directly used as an input to the first step. If the detected regime is *sticking*, some additional treatment is required to obtain an estimate of the frictional force λ_F which is then used as an input to the first step. These three steps are repeated till the value of λ_N in subsequent iterations is within a preset value. In each iteration, the value of λ_N is updated and consequently it is advisable to check if this affects the regime of motion calculated for the current contact. It has, however, been observed that, if the value of λ_N does not change by an order of magnitude, the calculated regime of motion does not change.

The iterative scheme described in this paper has some significant differences from the one presented in [9, 22]. The iterative approach presented in [9, 22] requires solving an LCP at each iteration and formulating the LCP is dependent on the type of integration method used. The iterative scheme presented in this paper does not require a traditional linear complementarity formulation. In effect, the iterative scheme ends up satisfying the same conditions as imposed by the linear complementarity formulation. On convergence, the first step of the scheme ensures that $0 \leq g_N \perp \lambda_N \geq 0$. For convergence, gradient information between g_N and λ_N is generated iteratively. The second and third steps ensure that, for the *sliding* regime, the direction of frictional force approximately opposes the relative tangential velocity at the point of contact during the course of the time step under consideration and for the *sticking* regime, frictional force applied is sufficient to prevent any relative tangential motion at the point of contact. The iterative scheme does not require discretization of the relative contact acceleration equations to obtain an expression for v_r^{l+1} (see (24)) which is an essential component of the LCP formulation. Any fixed time-step based higher order integration methods can be used with this scheme, since the value of the normal contact force and the corresponding frictional force are assumed/interpolated or generated iteratively which makes the problem of advancing the system from time t^l to t^{l+1} explicit. For an intermittent contact involving bodies with simple geometries, the use of higher order integration method also allows the use of larger time-steps which would normally result in significant errors in the traditional LCP formulations.

If there are multiple contacts in the system, each contact in the system is given a similar treatment. In the frictionless case, the iterative scheme is expected to give optimal results for multiple contacts. However, the multiple frictional contacts could potentially create scenarios in which the iterative scheme would either fail to converge or slow down significantly. This could happen due to frequent changes in the detected regimes of motion when the values of the normal contact forces are updated. This could potentially make the iterative scheme inadequate or inefficient for systems in the which a frictional contact is simultaneously possible between any combination of bodies within the system. However, the iterative scheme is ideally suited for a certain class of contact problems in robotics, biomechanics, MEMS and molecular dynamics, among others.

5 Numerical examples

In this section, some numerical examples are presented and a comparison is made between the results from the iterative scheme and traditional complementarity formulation for a rigid double pendulum. Then, a contact simulation of a two-link flexible robotic manipulator is described in which the traditional comple-

mentarity approach results in prohibitively small time-steps. This problem is, however, overcome on using the iterative scheme.

5.1 Iterative scheme

The iterative scheme is used to simulate a rigid 3D double pendulum [11] falling on a half-plane under the action of gravity as shown in Fig. 8. Body A and body B are connected via a spherical joint and a inelastic contact is defined between point P_1 on body A and the xy plane. Gravity acts along the negative z direction as shown in the figure. The fixed parameters of the system are as follows: $L_a = L_b = m_a = m_b = 1$, $I_a = I_b = \text{diag}(1, 2, 3)$, where I_a and I_b are the inertia matrices for bodies A and B respectively and *diag* is a diagonal matrix with the diagonal entries listed in the parentheses. The spatial orientation of the body is modeled using relative body-fixed *Euler-123* transformations.

In the first case, the spatial orientation vector of the system is set as $q_a = [0, 2, 0]$, $q_b = [2, 0, 0]$. The point P_1 is located at $(x, y, z) = (0, 0, 0)$ and the entire system is given an initial velocity $V_x = V_y = 1$. Coefficient of friction in this case is $\mu = 0.2$ and the system is simulated for 3 seconds. Figure 9 gives a plot of the orientation angles for both the bodies generated via a traditional LCP formulation, the iterative scheme described previously and Autolev. For the purpose of comparison, a first-order Euler integration is used in the iterative scheme. Next, to demonstrate the regimes of motion, the orientation vector of the system is set to $q_a = q_b = [0, 1, 0]$ and the system is released from rest with point P_1 located at $(x, y, z) = (0, 0, 0.1)$ and with the same coefficient of friction as in the previous case. The system is simulated for 30 seconds. As can be clearly seen from Fig. 10, the iterative scheme can capture different regimes of motion.

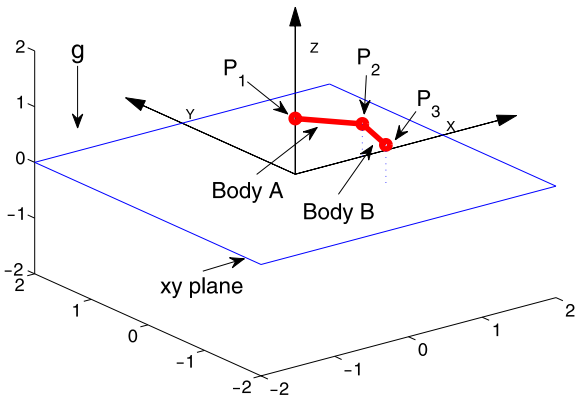

Fig. 8 Inelastic contact defined between point P_1 on body A and the xy plane

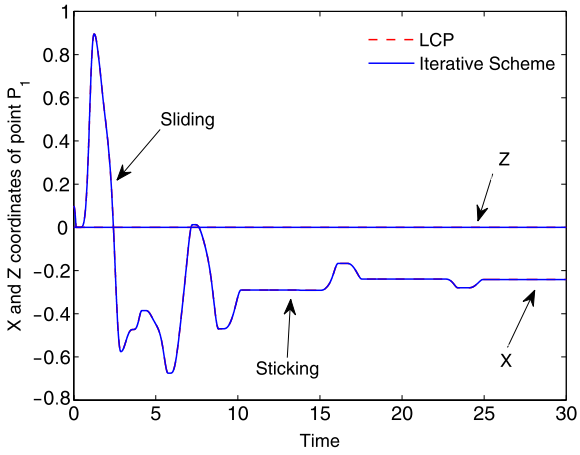

Fig. 10 Iterative scheme can capture transitions between different regimes of motion

Fig. 9 Comparison between traditional LCP formulation, iterative scheme and Autolev

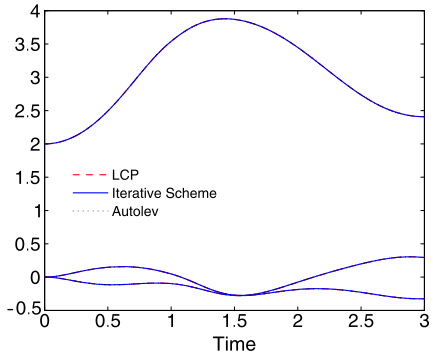

(a) Plot of orientation vector (q_a)for body A

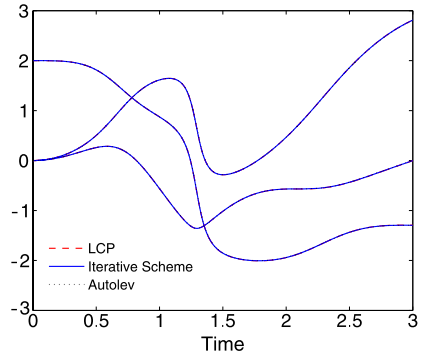

(b) Plot of orientation vector (q_b) for body B

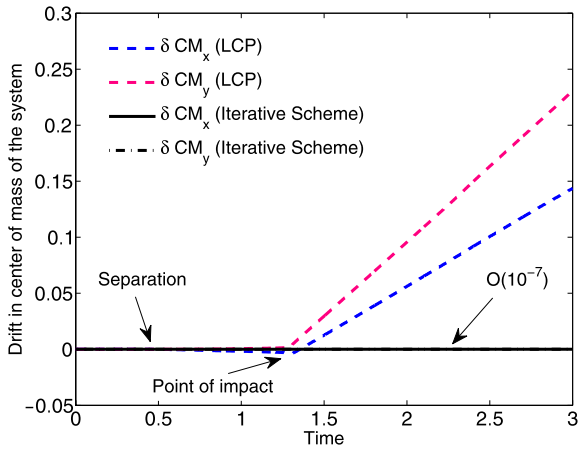

Fig. 11 Drift in x and y coordinates of the center of mass for the system for $\Delta t = 10^{-3}$ s

Next, to demonstrate an improvement in the solution, an explicit fixed time-step fourth order *Runge–Kutta* method is used with the iterative scheme. The orientation vector of the system is set as $q_a = [0, 2, 0]$, $q_b = [2, 0, 0]$ and coefficient of friction is set to zero. The system is released from rest with point P_1 located at $(x, y, z) = (0, 0, 1)$ and simulated for 3 seconds with $\Delta t = 10^{-3}$ s. Since there is no frictional force acting on the system, the center of mass of the system is not expected to move in x or y direction. Figure 11 gives the plot of the drift in the center of mass of the system calculated using the iterative scheme and an LCP formulation. The significant improvements in the results on using the iterative scheme can directly be explained by the integration scheme employed. As mentioned previously, the LCP formulation employs a first-order explicit Euler integration while the iterative scheme uses an fixed time-step fourth order *Runge–Kutta* integration.

5.2 Flexible robotic manipulator

The two-link robotic manipulator undergoing intermittent contact has already been simulated without a contact in [14, 25, 26] and shown in Fig. 12. All the joints in the system are revolute and the fixed parameters of the are as follows: $m_1 = 1$ kg, $L_1 = 0.545$ m, $E_1 = 7.3 \times 10^{10}$ N/m^2, $\rho_1 = 2700$ kg/m^3, $I_1 = 1.69 \times 10^{-8}$ m^{-4}, $A_1 = 9 \times 10^{-4}$ m^2, $m_2 = 3$ kg, $L_2 = 0.675$ m, $E_2 = 7.3 \times 10^{10}$ N/m^2, $\rho_2 = 2700$ kg/m^3, $I_2 = 3.33 \times 10^{-9}$ m^{-4}, $A_2 = 4 \times 10^{-4}$ m^2, $g = 9.81$ m/s^2, where all the symbols have the standard meaning.

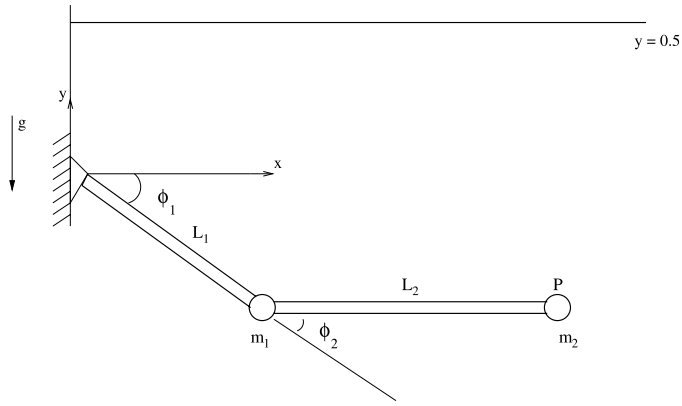

Fig. 12 Flexible robotic manipulator

A contact is defined between point P and the plane $y = 0.5$. The system starts from an undeformed configuration and undergoes a prescribed motion given in (27) for 0.5 seconds after which it is allowed to oscillate under the influence of gravity for 1.5 seconds.

$$\begin{aligned}\phi_1 &= -\pi/4 \cdots t < 0\\ &= \pi/4\left(-1 + 72t^3\right) \cdots 0 \le t < 1/6\\ &= \pi/4\left(-18t + 108t^2 - 144t^3\right) \cdots 1/6 \le t < 1/3\\ &= \pi/4\left(-8 + 54t - 108t^2 + 72t^3\right)\\ &\quad \cdots 1/3 \le t < 1/2\\ &= \pi/4 \cdots t > 1/2\\ \phi_2 &= -\phi_1. \end{aligned} \tag{27}$$

The modal shape functions used to model the deformation field within each body are given in (28). A single shape function is used to model the longitudinal and transverse deformations in each body.

$$\text{Longitudinal:} \quad (x/L)^2 \tag{28a}$$

$$\text{Transverse:} \quad 1.5(x/L)^2 - 0.5(x/L)^3. \tag{28b}$$

It should be noted that these shape functions are selected to conform with those describing a highly similar problem in the existing literature [14, 25, 26] and to demonstrate the proposed methods. This very limited set of shape functions will not generally be adequate for representing the deformation of the flexible bodies given the combined transverse loads, concentrated moments and axial loads which are experienced. In general, greater care is needed in the selection of

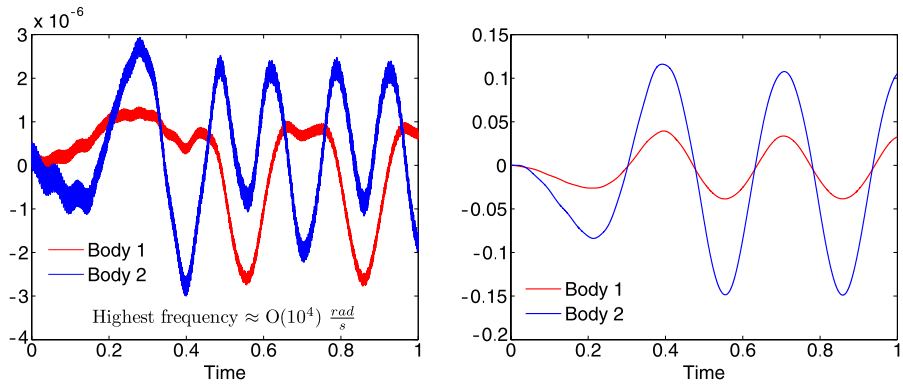

Fig. 13 Plot of modal coordinates without contact

(a) Longitudinal modal coordinate (b) Transverse modal coordinate

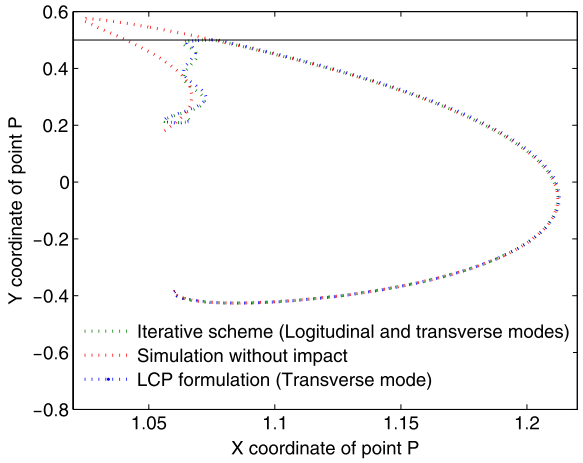

Fig. 14 Comparison between LCP formulation and the iterative scheme for fixed time-step $\Delta t = 10^{-4}$

acceptable set of shape functions so that the deformations are adequately captured without requiring and excessive number of modes. If the expected deformation in the elements is significant and grossly nonlinear, then it is preferable to use the absolute nodal coordinate formulation [27, 28]. In the current approach of using superposition of local mode shapes, it is possible to capture this large deformation by substructuring each link and using an adequate set of deformation modes.

Due to the nature of the problem and the selected mode shape functions, the longitudinal vibrations in each body are of a significantly higher frequency than the transverse vibrations. Figure 13 gives the plot of the modal coordinates of both the bodies when there is no contact. Geometric stiffness has been accounted for in all the simulations involving flexible bodies.

Due to the presence of the high frequency component in the longitudinal modal coordinates, the higher order terms in (24) are significant. As a first attempt, both the transverse and longitudinal deformation fields are included in the LCP formulation with $\Delta t = 10^{-4}$ s. It is observed that after the first impact, the simulation fails due to unrealistic value of the contact force computed by the LCP solver. This can be explained as follows. Suppose the contact occurs in the time step $t^l - t^{l+1}$. The computed contact force satisfies the complementarity conditions and the discretization given in (20). However, due to the presence of the high frequency longitudinal modal coordinates, their corresponding time derivatives are significant. Thus, the first-order approximation used (see (24)) in the expression for ${}^{l+1}\mathcal{V}_P$ is no longer accurate. This is evident, when ${}^{l+1}\mathcal{V}_P$ is recomputed from the updated values of the modal coordinates at time t^{l+1}. This recomputed value differs significantly from the corresponding value computed using (20) based on the contact force and the modal coordinates at time t^l. To alleviate this problem, the high frequency longitudinal component is eliminated and a single transverse deformation field is used. The contact force now obtained on impact is two orders of magnitude smaller than in the previous case. Indeed, the high frequency longitudinal component of the deformation field, in the selected test case, plays a minimal role in the global behavior of the entire system. However, it significantly affects the discretization of equations which are a necessary part of the LCP formulation. The iterative scheme discussed in previous section does not require discretization of any kind and hence both the transverse and longitudinal deformation fields can be used to simulate the impact. Figure 14 gives the plot of point P on impact us-

ing the iterative scheme and the LCP formulation. The iterative scheme used to generate the plot uses both the longitudinal and transverse components of the deformation field while the LCP formulation models could only be run successfully when using the low frequency transverse deformation field.

6 Conclusion

There are several engineering applications where one encounters the problem of simulating intermittent contact for flexible multibody systems. Certain applications like industrial assembly robots, MEMS devices and coarse-grain molecular systems, among others, are characterized by the presence of a large number of bilateral constraints in the system. The existing approach to deal with flexible multibody systems with intermittent contact results in either a large MCP or an expensive $O(n^3)$ calculation in dealing with system-wide mass matrix and the bilateral constraint equations to yield a minimal size LCP.

This paper presents a recursive scheme for flexible multibody systems involving intermittent contact resulting in a minimal size LCP at logarithmic cost for parallel implementation. The presented method is expected to be more efficient than other LCP approaches in presence of bilateral constraints in the systems. The recursive approach is an extension of the hybrid scheme for rigid bodies [11] to allow for small deformations within each body. The presented recursive scheme inherits all the properties of the underlying complementarity contact model and does not require a precise collision detection. The use of divide-and-conquer framework makes the scheme ideal for application to flexible multibody systems with different topologies.

The LCP contact formulation requires a first-order discretization to obtain an expression for the relative contact velocity at time t^{l+1} based on the state at time t^l. This could be undesirable in certain class of problems involving flexible bodies. Additionally, the traditional LCP approach does not allow the use of higher order integration scheme. To overcome these issues, an iterative scheme is presented which does not require a traditional LCP formulation. The contact force values are initially assumed and iteratively updated, which makes the problem of advancing the simulation from time t^l to t^{l+1} explicit. This allows the use of any fixed time-step based higher order integration routine with the iterative scheme. The iterative scheme is insensitive to the high frequency components in the state vector of the system and is expected to be optimal for multibody systems involving relatively fewer contacts. Additionally, in applications involving contact between bodies with relatively simple geometries, this alternative approach allows the use of larger time-steps and demonstrates improved accuracy, when compared to the more traditional LCP formulations.

Acknowledgements This work was supported by NSF grant No. 0555174. The authors gratefully acknowledge this support.

References

1. Wriggers, P.: Finite element algorithms for contact problems. Arch. Comput. Methods Eng. **2**(3), 1–49 (1995)
2. Hunt, K., Crossley, F.: Coefficient of restitution interpreted as damping in vibroimpact. ASME J. Appl. Mech. **42**, 440–445 (1995)
3. Pereira, M.S., Nikravesh, P.: Impact dynamics of multibody systems with frictional contact using joint coordinates and canonical equations of motion. Nonlinear Dyn. **9**, 53–71 (1996)
4. Pfeiffer, F.: The idea of complementarity in multibody dynamics. Arch. Appl. Mech. **72**(11–12), 807–816 (2003)
5. Trinkle, J., Zeng, D., Sudarsky, S., Lo, G.: On dynamic multi-rigid-body contact problems with Coulomb friction. Z. Angew. Math. Mech. **77**(4), 267–279 (1997)
6. Barhorst, A.A.: On modelling variable structure dynamics of hybrid parameter multibody systems. J. Sound Vib. **209**(4), 571–592 (1998)
7. Pfeiffer, F.B., Glocker, C.: Multibody Dynamics with Unilateral Contacts. Wiley Series in Nonlinear Sciences. Wiley, New York (1996)
8. Foerg, M., Pfeiffer, F., Ulbrich, H.: Simulation of unilateral constrained systems with many bodies. Multibody Syst. Dyn. **14**, 137–154 (2005)
9. Ebrahimi, S.: A contribution to computational contact procedures in flexible multibody systems. Ph.D. thesis, University of Stuttgart (2007)
10. Ebrahimi, S., Eberhard, P.: On the use of linear complementarity problems for contact of planar flexible bodies. In: Proceedings of the ECCOMAS Thematic Conference on Multibody Dynamics, Madrid, Spain (2005)
11. Bhalerao, K.D., Anderson, K.S., Trinkle, J.C.: A recursive hybrid time-stepping scheme for intermittent contact in multi-rigid-body dynamics. J. Comput. Nonlinear Dyn. **4**(4), 041010 (2009)
12. Shabana, A.: Flexible multibody dynamics: Review of past and recent developments. Multibody Syst. Dyn. **1**(2), 189–222 (1997)
13. Schwertassek, R., Wallrapp, O., Shabana, A.: Flexible multibody simulation and choice of shape functions. Nonlinear Dyn. **20**(4), 361–380 (1999)

14. Mukherjee, R., Anderson, K.S.: A logarithmic complexity divide-and-conquer algorithm for multi-flexible articulated body systems. Comput. Nonlinear Dyn. **2**(1), 10–21 (2007)
15. Featherstone, R.: A divide-and-conquer articulated body algorithm for parallel $O(\log(n))$ calculation of rigid body dynamics. Part 1: Basic algorithm. Int. J. Robotics Res. **18**(9), 867–875 (1999)
16. Featherstone, R.: A divide-and-conquer articulated body algorithm for parallel $O(\log(n))$ calculation of rigid body dynamics. Part 2: Trees, loops, and accuracy. Int. J. Robotics Res. **18**(9), 876–892 (1999)
17. Mukherjee, R., Anderson, K.S.: An orthogonal complement based divide-and-conquer algorithm for constrained multibody systems. Nonlinear Dyn. **48**(1–2), 199–215 (2007)
18. Kane, T.R., Levinson, D.A.: Dynamics: Theory and Application. McGraw-Hill, New York (1985)
19. Stewart, D.E., Trinkle, J.C.: An implicit time-stepping scheme for rigid body dynamics with inelastic collisions and coulomb friction. Int. J. Numer. Methods Eng. **39**, 2673–2691 (1996)
20. Escalona, J., Mayo, J., Dominguez, J.: A critical study of the use of the generalized impulse-momentum balance equations in flexible multibody systems. J. Sound Vib. **217**(3), 523–545 (1998)
21. Escalona, J., Sany, J., Shabana, A.: On the use of the restitution condition in flexible body dynamics. Nonlinear Dyn. **30**, 71–86 (2002)
22. Ebrahimi, S., Eberhard, P.: A linear complementarity formulation on position level for frictionless impact of planar deformable bodies. Z. Angew. Math. Mech. **86**(10), 808–817 (2006)
23. Mukherjee, R.M., Anderson, K.S.: Efficient methodology for multibody simulations with discontinuous changes in system definition. Multibody Syst. Dyn. **18**, 145–168 (2007)
24. Mukherjee, R.M., Anderson, K.S.: A generalized momentum method for multi-flexible body systems for model resolution change. In: Proceedings of the 12th Conference on Nonlinear Vibrations, Dynamics, and Multibody Systems. Blacksburg, VA (2008)
25. Botz, M., Hagedorn, P.: Dynamic simulation of multibody systems including planar elastic beams using autolev. Eng. Comput. **14**(4), 456–479 (1997)
26. Claus, H.: A deformation approach to stress distribution in flexible multibody systems. Multibody Syst. Dyn. **6**, 143–161 (2001)
27. Shabana, A.A., Yakoub, R.Y.: Three dimensional absolute nodal coordinate formulation for beam elements: Theory. J. Mech. Des. **123**(4), 606–613 (2001)
28. Yakoub, R.Y., Shabana, A.A.: Three dimensional absolute nodal coordinate formulation for beam elements: Implementation and applications. J. Mech. Des. **123**(4), 614–621 (2001)